

Dielectric Properties of BaTiO₃ Single Crystals in the Paraelectric State from 1 kc/sec to 2000 Mc/sec

E. STERN AND ALLEN LURIO

International Business Machines Watson Laboratory, Columbia University, New York, New York

(Received January 27, 1961)

The dielectric constant of BaTiO₃ single crystals in the region above the 120°C Curie point has been measured at several frequencies in the range from 1 kc/sec to 2000 Mc/sec. In addition, the B coefficient in Devonshire's equation for the free energy has been studied at 500 Mc/sec. It is shown that the crystal is completely clamped with respect to the measuring field at 500 Mc/sec so that the coefficient of the P^4 term in Devonshire's equation is positive and agrees with the expected theoretical result of $B_F^C = 2.23 \times 10^{-13}$ cgs unit.

INTRODUCTION

PREVIOUS studies of BaTiO₃ at low frequencies have described the variation of the dielectric constant ϵ' as a function of temperature.¹ At the ferroelectric Curie temperature of 120°C, a discontinuous transition takes place between the ferroelectric and the paraelectric state. Above this temperature T_c , the crystal is in the paraelectric state and the dielectric constant follows a Curie-Weiss law $\epsilon' = 4\pi/[2A(T - T_0)]$. A property of the material, one that makes it attractive in numerous applications, is the variation of the dielectric constant under the influence of an electric biasing field.

Devonshire² developed a phenomenological theory by which he explained the ferroelectric behavior of BaTiO₃. He started by expanding the free energy of a stress-free crystal and obtained an equation which in the region above the 5° C transition point reduces to

$$F(P; T) = F(0, T) + A(T - T_0)P^2 + BP^4 + CP^6, \quad (1)$$

where A , B , and C are constants, P is the polarization along the tetragonal axis, T is the temperature, and $F(0, T)$ is the free energy at zero polarization.

Various observers have reported on low frequency measurements of the dielectric properties of BaTiO₃ single crystals. Merz,³ and Drougard, Landauer and Young⁴ have reported experimental values for the A , B , and C constants in (1). Results at 10 kc/sec show that ϵ' reaches a peak value as high as 15 000 at the Curie point.⁵

Recently, measurements of ϵ' in the paraelectric region have been extended to X and K band frequencies^{6,7} and yield results similar to those at 10 kc/sec. There has not been, however, any measurements of the B coefficient in (1) at frequencies above 10 kc/sec. We will present in this paper measurements of the

dielectric constant of BaTiO₃ in the region from 1 kc/sec to 2000 Mc/sec, and a measurement of the B coefficient at 500 Mc/sec and at 1 kc/sec.

THEORETICAL BACKGROUND

We follow a treatment analogous to that of Devonshire and define a Gibbs function G , where

$$G = F - EP, \quad (2)$$

which describes the energy of BaTiO₃ over its entire temperature range. In this equation, F is the Helmholtz free energy, E is the externally applied electric field, and P is the polarization of the crystal. Since we are looking for the stable states of the material, G must be a minimum, so that at a constant temperature,

$$(\partial G / \partial P)_T = 0 = (\partial F / \partial P) - E, \quad (3)$$

and

$$(\partial^2 G / \partial P^2)_T = \partial^2 F / \partial P^2 > 0, \quad (4)$$

In order to obtain the dielectric constant of the crystal, we make use of the relation

$$\partial E / \partial P = 4\pi / (\epsilon' - 1) \approx (4\pi / \epsilon'), \quad (5)$$

where ϵ' is the relative dielectric constant. Below the Curie temperature T_c where the crystal has a spontaneous polarization, we have from (5), (3), and (1)

$$(4\pi / \epsilon') = 2A(T - T_0) + 12BP^2 + 30CP^4, \quad (6)$$

whereas above T_c where $P = 0$

$$(4\pi / \epsilon_0') = 2A(T - T_0). \quad (7)$$

ϵ_0' is the dielectric constant at zero polarization. Actually, the transition to the ferroelectric state is found to occur above the temperature T_0 , namely at T_c the Curie temperature, where P changes discontinuously to zero. Therefore, the dielectric constant is finite though discontinuous at the Curie point.

Equation (7) shows that ϵ_0' follows a Curie-Weiss law above T_c . From it, the A constant in (1) can be determined.

The electric biasing fields used in this experiment were chosen of such a magnitude as to make the CP^4 term in (6) negligible compared to the BP^2 term. Thus,

$$4\pi / \epsilon' \cong 2A(T - T_0) + 12BP^2. \quad (8)$$

¹ W. Kanzig, *Advances in Solid State Physics* (Academic Press, Inc., New York, 1957), Vol. 4, pp. 1-197.

² A. F. Devonshire, *Phil. Mag.* **3**, 10, 85-130S (1954).

³ W. J. Merz, *Phys. Rev.* **91**, 513 (1953).

⁴ M. E. Drougard, R. Landauer, and D. R. Young, *Phys. Rev.* **98**, 1010 (1955).

⁵ M. E. Drougard and D. R. Young, *Phys. Rev.* **95**, 1152 (1954).

⁶ T. S. Benedict and J. L. Durand, *Phys. Rev.* **109**, 1091 (1958).

⁷ A. Lurio and E. Stern, *J. Appl. Phys.* **31**, 1805 (1960).

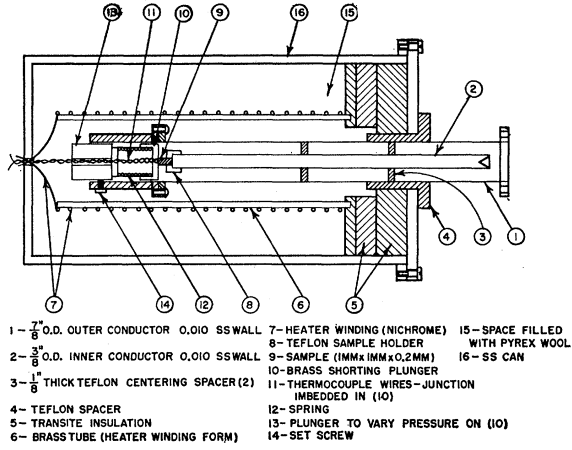


FIG. 1. Schematic drawing of dielectrometer cell.

In this equation the polarization P is due to the externally applied field since above T_c the spontaneous polarization is zero. If we introduce (7) into the above equation, we get

$$(4\pi/\epsilon') - (4\pi/\epsilon'_0) = 12BP^2. \quad (9)$$

We can now combine Eqs. (1), (3), and (7) to obtain

$$E = (4\pi P/\epsilon'_0) + 4BP^3, \quad (10)$$

and with Eq. (9) this may be written as

$$B = (16\pi^3/27E^2)[(1/\epsilon') - (1/\epsilon'_0)][(2/\epsilon'_0) + (1/\epsilon')], \quad (11)$$

enabling one to determine B from the experimental data.

The meaning of B as obtained above is unambiguous if we are dealing with a crystal entirely free of stresses. BaTiO_3 , however, is electrostrictive in the paraelectric region, and undergoes dimensional changes upon the application of polarizing fields. It has been suggested^{2,4} that at frequencies higher than the piezoelectric resonance, the crystal finds itself completely clamped with respect to the measuring field, though it is still free to respond to the large and slow variations of the biasing field. How BaTiO_3 single crystals behave when certain stresses are present to hinder these electrostrictive strains has been treated in detail by Drougard, Landauer, and Young⁴ (henceforth referred to as DLY).

We follow the notation of DLY in which ϵ' and the B coefficient are more completely identified as $\epsilon'_x{}^y$ and $B_x{}^y$, x referring to the condition of the crystal with respect to the biasing voltage and y referring to the measuring voltage. Thus for example, $B_F{}^C$ refers to a crystal clamped with respect to the measuring field but free with respect to the biasing voltage.

DLY start from a more general free energy function,

$$F(P, T, x_i) = \frac{1}{2}c_{11}(x_1^2 + x_2^2 + x_3^2) + c_{12}(x_1x_2 + x_2x_3 + x_3x_1) + A(T - T_0)P^2 + B_C{}^C P^4 + g_{11}x_3P^2 + g_{12}(x_1 + x_2)P^2, \quad (12)$$

where c_{11} and c_{12} are stiffness coefficients, the x_i are strains, and g_{11} and g_{12} measure the coupling between

the crystal strain and the polarization. They then proceed to investigate the case of a crystal free from stresses, the case of a crystal completely clamped longitudinally, and the case of a crystal still longitudinally clamped with respect to the measuring voltage but free with respect to the biasing field.

Since the stresses are defined by the relation $X_i = -(\partial F_i / \partial x_i)$, it follows that $(\partial F_i / \partial x_i) = 0$ for the case of a totally free crystal. Hence, the x_i are functions of P^2 and from (3) we have

$$E = 2A(T - T_0)P + 4B_C{}^C P^3 + 2g_{11}x_3P + 2g_{12}(x_1 + x_2)P. \quad (13)$$

The free dielectric constant $\epsilon_F{}^F$ is obtained by differentiating E with respect to P , so that

$$(4\pi/\epsilon_F{}^F) = 2A(T - T_0) + 12B_C{}^C P^2 + 2g_{11}x_3 + 2g_{12}(x_1 + x_2) + 2g_{11}P(dx_3/dP) + 2g_{12}P[(dx_1/dP) + (dx_2/dP)]. \quad (14)$$

Since the crystal can strain freely, $(dx_i/dP) \neq 0$ and DLY show that

$$(dx_i/dP) = (2x_i/P) \quad \text{for a free crystal.} \quad (15)$$

Hence,

$$(4\pi/\epsilon_F{}^F) = 2A(T - T_0) + 12B_C{}^C P^2 + 6g_{11}x_3 + g_{12}(x_1 + x_2), \quad (16)$$

and it follows from (8) that

$$B_F{}^F = B_C{}^C + (1/2P^2)[g_{11}x_3 + g_{12}(x_1 + x_2)]. \quad (17)$$

In the present work the frequency of the measuring voltage has been increased beyond the region of the piezoelectric response, thus subjecting the crystal to complete clamping with respect to the measuring voltage. The crystal may still respond to the slowly varying biasing field. Under such conditions, in the notation of DLY, $d'x_i = 0$, where $d'x_i$ are the differential strains induced by the measuring field under a strain condition x_i induced by the biasing field and we obtain

$$(4\pi/\epsilon_F{}^C) = 2A(T - T_0) + 12B_C{}^C P^2 + 2g_{11}x_3 + 2g_{12}(x_1 + x_2), \quad (18)$$

and, thus,

$$B_F{}^C = B_C{}^C + (1/6P^2)[g_{11}x_3 + g_{12}(x_1 + x_2)]. \quad (19)$$

This can be rewritten by use of Eq. (17) so that

$$B_F{}^C = B_F{}^F - (1/3P^2)[g_{11}x_3 + g_{12}(x_1 + x_2)]. \quad (20)$$

Triebwasser has shown⁸ that $B_C{}^C = B_F{}^F + 7.1 \times 10^{-13}$ cgs unit. Hence, from Eq. (17) we see that

$$(1/2P^2)[g_{11}x_3 + g_{12}(x_1 + x_2)] = -7.1 \times 10^{-13},$$

which in turn leads to

$$B_F{}^C = B_F{}^F + 4.73 \times 10^{-13} \text{ cgs unit.} \quad (21)$$

⁸ S. Triebwasser, J. Phys. Chem. Solids 3, 53 (1957).

The results of the DLY experiment indicated that $B_F^F = -2.5 \times 10^{-13}$ cgs units at the Curie point. If the crystal is indeed clamped by the microwave measuring field used in our experiment, we should measure $B_F^C = +2.23 \times 10^{-13}$ cgs units at the Curie temperature. This type of behavior would be characteristic of a second-order transition, as predicted by Devonshire.

Our interest in this experiment was centered on the temperature region above the Curie point. This region is of more practical interest in that ferroelectric losses are not present to hinder high-frequency applications.

DESCRIPTION OF DIELECTROMETER

The experimental arrangement described in Fig. 1 is similar to that used by Jaynes and Varenhorst.⁹ The measuring cell consisted of a $\frac{7}{8}$ -in. o.d. coaxial line with a characteristic impedance Z_0 of 50 ohms, which was terminated by the BaTiO₃ sample. The coaxial sample holder assembly was enclosed in a cylindrical oven to permit measurements in the range from room temperature to about 180°C.

The BaTiO₃ samples were single crystals $1 \times 1 \times 0.25$ mm, with evaporated gold electrodes on opposite 1×0.25 -mm faces. A Teflon cap with an *H*-shaped slit across the face was fitted over the center conductor of the coaxial line; the sample was held in the slit. One electrode of the crystal made contact with the end of the center conductor; the other, with the end of a spring-loaded shorting plunger.

An iron-constantan (type *J*) thermocouple T_1 was imbedded in the thin face of the plunger to measure the temperature of the sample. The spring behind the piston-like short circuit always kept it in contact with the crystal. Care had to be taken that the pressure be kept relatively constant through the whole temperature range to maintain good electrical contact with the electrodes. On the other hand, if the pressure were excessive, the crystal could easily be damaged. This was especially critical at the transition temperature where the sample rapidly undergoes large dimensional changes. Excessive resistance to these changes would cause the sample to shatter.

Thin-wall (0.010 in.) stainless steel tubing was used in the construction of the coaxial line. This was done in order to minimize heat losses through the line. An additional thermocouple T_2 was installed inside the center conductor, at the end nearest the sample. The thermocouple junctions located on opposite ends of the specimen permitted the measurement of temperature gradient $\Delta T = T_2 - T_1$ across the sample. The temperature of thermocouple T_2 could not be monitored during a run, however, since this interfered with the rf properties of the coaxial line. A heavy brass slug at the sample end of the center conductor and a brass collar around the same end of the outer conductor helped in maintaining $\Delta T < 1^\circ\text{C}$ above the Curie temperature.

⁹ E. T. Jaynes and V. Varenhorst, Microwave Lab Report No. 287, Stanford University, Stanford, California (unpublished).

The oven was insulated with Pyrex wool. Its temperature was controlled by varying the voltage on a heater winding surrounding the coaxial line. Measurements were made as the temperature drifted down at a rate of approximately 10°C/hr through the range of interest, namely 160°C to 115°C . The temperature was monitored by reading the thermocouple voltage T_1 on a Rubicon potentiometer.

MEASUREMENT PROCEDURE

Each sample was calibrated at 1 kc/sec by measuring its capacitance and $\tan\delta$ as a function of temperature. These curves provided a reference to which the high-frequency data could be compared. For this measurement, a Beco impedance bridge was connected directly to the dielectrometer line. The capacitance and $\tan\delta$ of the sample could be read off the bridge dials as a function of temperature.

In the vhf region, a Boonton 190-A *Q* meter was used. Here again, both the capacitance and *Q* of the sample could be read directly from meter dials. Above 40 Mc/sec, however, corrections for line length became appreciable and had to be taken into account. From transmission line theory, the load admittance Y_L of a reactive network in terms of its input admittance Y_{in} , for a line of length *l*, is

$$Y_L = Y_0(Y_{in} - jY_0 \tan\beta l) / (Y_0 - jY_{in} \tan\beta l), \quad (22)$$

where Y_0 = characteristic admittance of the line = 2×10^{-2} ohm⁻¹ and $\beta = 2\pi/\lambda$. For the equivalent circuit chosen to represent our sample as discussed in the following section, the input admittance of the sample is

$$Y_{in} = G_s + j\omega C_s = \omega C_0 [(1/Q_2) - (1/Q_1)] + j\omega(C_2 - C_1), \quad (23)$$

where C_0 = capacitance at the open *Q*-meter terminals; C_1 , Q_1 = capacitance and *Q* with empty test line; C_2 , Q_2 = capacitance and *Q* with sample in test line.

The first step in the procedure consists of measuring C_0 and Q_0 with the *Q*-meter terminals open. The line is then attached not containing a sample; this yields the value C_1 , the fringing capacitance of the gap; and Q_1 , the line losses. The crystal is then inserted and C_2 and Q_2 are measured as a function of temperature, and frequency.

At 500 Mc/sec and above, a slotted-line technique was used. The shift of the VSW (Voltage Standing Wave) minimum and the magnitude of the VSWR (Voltage Standing Wave Ratio) σ in an HP805-B $\frac{7}{8}$ in. coaxial slotted line are sufficient to determine the change in capacitance and $\tan\delta$ of the sample. General Radio unit oscillators provided rf power up to 2000 Mc/sec; above 2000 Mc/sec, a 2K41 klystron was used. The detected output voltage from the slotted-line probe was read on an HP425-Amicrovolt-ammeter. The crystal detector was initially calibrated for voltage vs

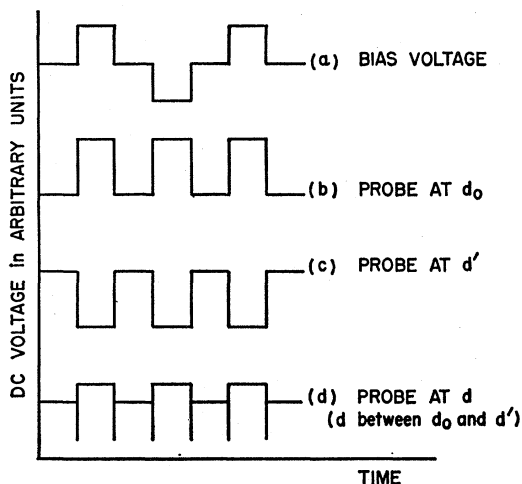


FIG. 2. Bias and probe wave forms expected theoretically. The intercept of the wave forms with the vertical axis occurs at the condition of zero bias voltage.

power law and its deviation from square-law behavior was accounted for in the evaluation of the data.

In performing the measurements, a brass replica of the sample was first placed into the Teflon holder and the position of the first minimum d_0 of the standing wave in the slotted-line was measured. This represents a point of infinite capacitance which establishes a reference plane at a particular frequency.⁹ The VSWR σ was also measured. Similar measurements were made on the empty test line to give the fringing capacitance and line losses. With the crystal in place, σ and the variation of the position d of the standing wave minimum with respect to d_0 , namely $d - d_0$, were recorded as a function of temperature.

The impedance of the sample Z_L is then found in terms of σ and d from the relation⁹

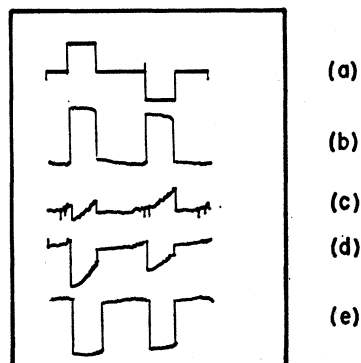


FIG. 3. Bias and probe wave forms observed experimentally. This is a copy of a photograph depicting the biasing voltage applied to the BaTiO_3 crystal and the progressive change in the pattern detected on the oscilloscope as the standing wave detector probe is moved from d to d' . (a) Biasing voltage ± 500 v. (b) Probe at d [position of VSW minimum without bias]. (c), (d) Probe between d and d' . (e) Probe at d' [position of VSW minimum shifted by the bias]. This photograph was taken at a crystal temperature of 127°C .

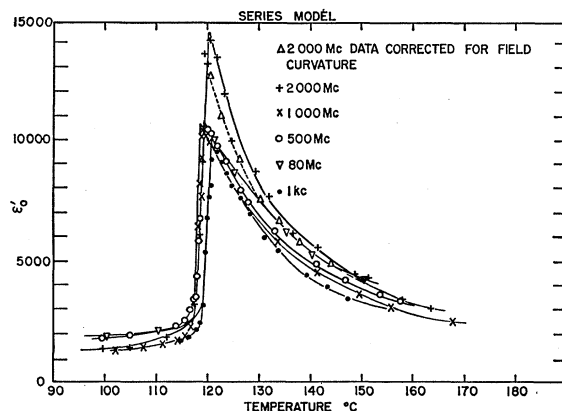


FIG. 4. Series model: relative dielectric constant vs temperature.

$$Z_L = Z_0 \left[\frac{\sigma(1+T^2)}{\sigma^2+T^2} - j \frac{T(\sigma^2-1)}{\sigma^2+T^2} \right], \quad (24)$$

where $T = \tan[\beta(d - d_0)]$. This procedure was repeated at a number of frequencies. The frequency was monitored by (a) measuring the wavelength in the slotted line, and (b) comparing the signal with the harmonics of a 1-Mc/sec frequency standard.

In order to measure the B coefficient, a variable high voltage square wave generator was designed. It provided a 20–60 cps pulsed wave [see Fig. 2(a)] across the sample, of amplitude ranging from 0 to 500 v. Due to the change in the dielectric constant with applied voltage (a change proportional to the square of the voltage) the position of the VSW minimum shifts at a rate twice that of the applied voltage (i.e., 40–120 cps) with respect to the position of the VSW minimum d_0 at zero voltage; the direction of the shift is independent of the polarity of the applied voltage. The slotted line probe voltage for this condition is shown in Fig. 2(b). If d' is the new VSW minimum at the maximum and minimum of the applied dc voltage then the expected probe voltage waveform is shown in Fig. 2(c). For the probe intermediate between these positions, the expected probe waveform is shown in Fig. 2(d). The output of the probe detector was displayed on a high-gain dc oscilloscope. A photograph of the scope patterns observed is shown in Fig. 3 as the probe is moved from d_0 to d' . From the photographs one sees that the probe voltage is not identical during the positive and negative maxima of the biasing voltage; however, the two probe voltage minima occur at the same probe position d' . This asymmetry has not been explained.

RESULTS AND DISCUSSION

The sample in the dielectrometer line can be represented by a two-terminal network composed of lumped resistive and reactive components. We have seen that the experiment consisted essentially of measuring the impedance or admittance of the sample as a function

of temperature, frequency, and biasing voltage. At any one frequency, a number of combinations of R and X will result in the same value for Z_L . The simplest equivalent circuits of the sample would be those resulting from placing an ideal capacitance C in series or in parallel with a resistance R . By comparing the frequency response of either circuit with that observed in the dielectric, one can choose the appropriate equivalent representation.

The impedance of the test line may be described by a parallel RC circuit for which the input admittance

$$Y_{in}^P = G_{in}^P + j\omega C_{in}^P = \frac{\omega C_{in}^P}{Q} + j\omega C_{in}^P \\ = \omega C_{in}^P \tan\delta + j\omega C_{in}^P. \quad (25)$$

This parallel RC network is easily related to the series RC network if we use the fact that the real and imaginary parts of the series and parallel admittances are respectively equal. For the series RC circuit the input impedance

$$Z_{in}^S = R_{in}^S - (j/\omega C_{in}^S). \quad (26)$$

It then follows that

$$\tan\delta = \omega C_S R_S. \quad (27)$$

$$R_S = \{ \tan\delta / C_P [(\tan\delta)^2 + 1] \} \quad (28)$$

and

$$\{ C_S = C_P [(\tan\delta)^2 + 1] \}. \quad (29)$$

It is seen that in the limit where $\tan\delta$ is small (in our case, at low frequencies or high temperatures), $C_P = C_S$.

Below 50 Mc/sec, where the length of line l is short compared to a wavelength, the crystal capacitance C_S is easily derived from instrument dial readings. The loss tangent, as derived in the Appendix, is given by

$$\tan\delta_S = [C_0 / (C_1 - C_2)] [(1/Q_2) - (1/Q_1)]. \quad (30)$$

With our experimental arrangement, at frequencies above 50 Mc/sec, line length corrections had to be applied to the admittances as obtained from the Q -meter readings. If $Y = G + jB$ is the admittance for

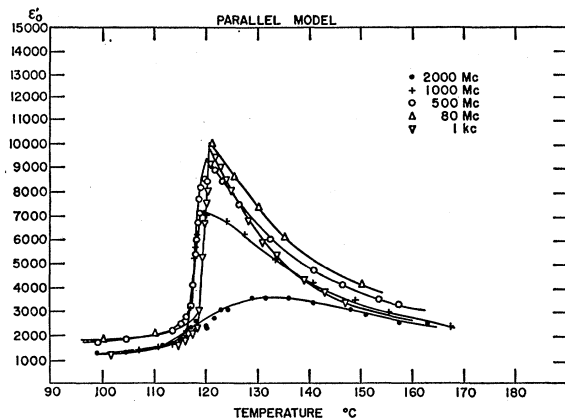


FIG. 5. Parallel model: relative dielectric constant vs temperature.

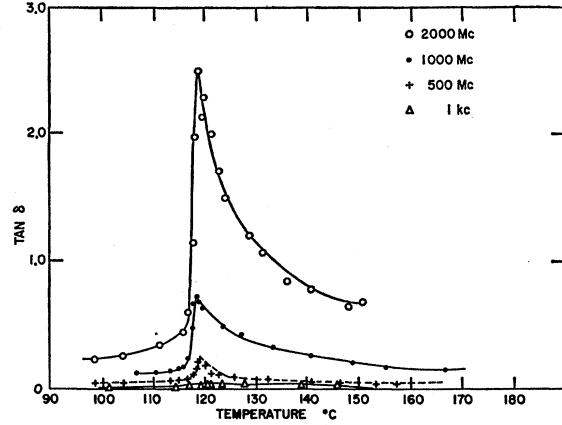


FIG. 6. Loss tangent vs temperature.

Q -meter readings C and Q and the primed quantities refer to the transformed admittances, then it follows that

$$C_S = [(B_2 - B_0)' - (B_1 - B_0)'] / \omega, \quad (31)$$

and

$$\tan\delta_S = [(G_2 - G_0)' - (G_1 - G_0)'] / [(B_2 - B_0)' - (B_1 - B_0)'].$$

In view of the well-known difficulties in obtaining low Ohmic resistance between the crystal face and an evaporated electrode of silver or gold, we were prompted to choose a series circuit to represent the sample terminating the coaxial line. Examination of the high-frequency data supported this assumption (see Figs. 5 and 7). When interpreting the slotted line measurements from 500–2500 Mc/sec, we use the relation

$$Z_L = \frac{Z_{in} - jZ_0 \tan\beta(d - d_0)}{Z_0 - jZ_{in} \tan\beta(d - d_0)} = R + jX \quad (32)$$

and the definition

$$\sigma = (Z_0 / Z_{in}) \quad (33)$$

to arrive at Eq. (24) above. Hence the loss tangent of the sample is given by

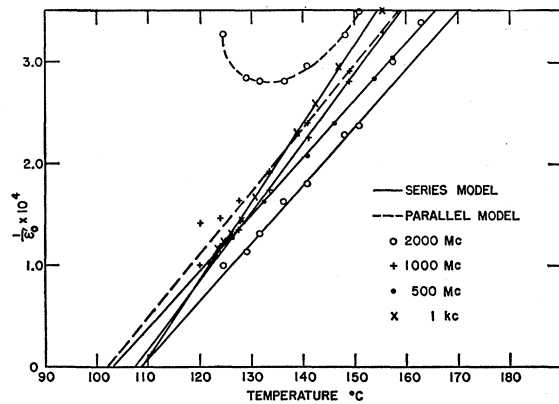
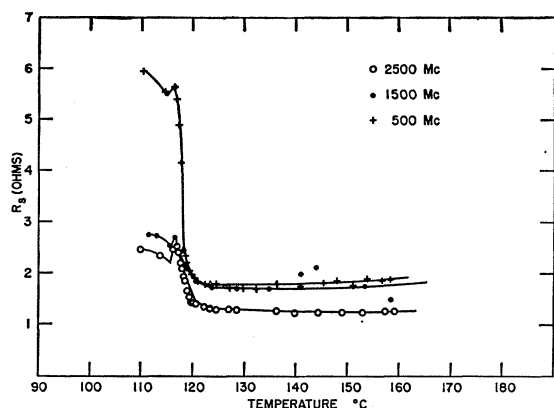


FIG. 7. Curie-Weiss law behavior.

FIG. 8. R_s (series model resistance) vs temperature.

$$\tan\delta = -\frac{R}{X} \frac{\sigma(1+T^2)}{T(\sigma^2-1)} \approx \frac{1+T^2}{\sigma T} \quad \text{for large } \sigma, \quad (34)$$

and since $X = -(1/\omega C_s)$,

$$C_s = \frac{1}{Z_0 \omega} \frac{\sigma^2 + T^2}{T(\sigma^2 - 1)} \approx \frac{1}{Z_0 \omega} \frac{\sigma^2 + T^2}{T \sigma^2}. \quad (35)$$

The dielectric constant comes out of Eqs. (31) and (35) by assuming the sample to be a parallel plane capacitor, for which

$$\epsilon' = (t/A \epsilon_0) C, \quad (36)$$

where t = length of sample in meters, A = area of electrodes in (meters)², $\epsilon_0 = 8.854 \times 10^{-12}$ farad/meter, and C = capacitance of sample as computed from Eqs. (31) and (35). Equation (36) gives correct results up to approximately 1000 Mc/sec. At 2000 Mc/sec, as large as a 15% error is introduced by the field curvature effect (the variation of the electric field along the thin dimension of the crystal). This effect was treated in detail by Jaynes.⁹ It causes the measured dielectric constant to appear higher than its actual value.¹⁰

An IBM 650 computer was used to reduce the data. The results which are plotted in Figs. 4-7 were obtained from the same crystal and are representative of the

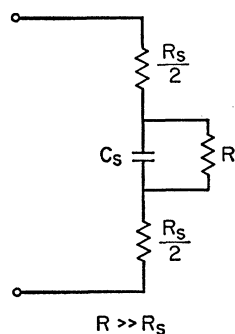


FIG. 9. Circuit representing sample.

TABLE I. Experimental values of the peak dielectric constant ϵ' , A in Devonshire's free-energy equation, and T_0 in the Curie-Weiss law $\epsilon' = [2\pi/A(T-T_0)]$ as functions of frequency.

Frequency	Peak ϵ'	A ($^{\circ}\text{C}$) ⁻¹	T_0 ($^{\circ}\text{C}$)
1 kc/sec	10 000	3.29×10^{-5}	105.1 $^{\circ}$
20 Mc/sec	10 000	3.27×10^{-5}	106.5 $^{\circ}$
80 Mc/sec	10 000	2.7×10^{-5}	100 $^{\circ}$
500 Mc/sec	10 500	3.6×10^{-5}	104 $^{\circ}$
1000 Mc/sec	10 200	4.34×10^{-5}	107.2 $^{\circ}$
2000 Mc/sec	13 500	3.71×10^{-5}	109.3 $^{\circ}$

results obtained from a number of crystals, five of which yielded data over the entire frequency range without shattering. The data taken below the Curie temperature are also presented in the figures but are not discussed since the crystals are probably multi-domain in that region. Figure 4 shows ϵ'_0 vs temperature at a number of frequencies for the series model equivalent circuit (see Fig. 9). Most of the apparent increase in the dielectric constant at 2000 Mc/sec can be accounted for by the field curvature effect mentioned above; the remainder is probably due to the uncertainty in locating the position of the standing wave minimum.¹⁰ This uncertainty becomes more important as the measuring frequency increases, since the total shift in the position of the minimum decreases with increasing frequency. Table I contains a summary of the constants in the Curie-Weiss law for the series model obtained from the curves in Fig. 7. In Fig. 8 is plotted the resistance R_s which in the paraelectric region is observed to stay remarkably constant with temperature at frequencies above 500 Mc/sec. This fact and a consideration of the curves in Figs. 5 and 7 provide the basis for choosing the series model for the equivalent circuit. The rapidly increasing value of $\tan\delta$ as a function of frequency (see Fig. 6) is also consistent with this model. At 1 kc/sec where R_s is negligible compared to the high reactance of C_s , the parallel resistance R (see Fig. 9) representing the bulk losses in the sample was determined to be on the order of 10^8 ohms.

In Fig. 10, the dielectric constant at 500 Mc/sec is plotted as a function of temperature for a number of values of biasing voltage applied across the sample. The crystal used in these measurements is not the same as that one used to obtain the curves in Figs. 4-7. It is evident from the curves in Fig. 10 that the dielectric constant decreases with applied biasing voltage. The B_F^C coefficient (see Fig. 11) derived from these curves varies between 2.1×10^{-13} and 3.7×10^{-13} cgs units over the temperature range from 120 $^{\circ}$ to 130 $^{\circ}$ C. This is in excellent agreement with the theoretically predicted value and leads us to believe that at these high frequencies, BaTiO₃ crystals are completely clamped with respect to the measuring field and indeed undergo a second-order transition.

As an additional check, we tested a crystal at 1 kc/sec and found that the B_F^F coefficient was -2.5×10^{-13} cgs

¹⁰ Note added in proof. In addition, this apparent increase in ϵ may be associated with the approach toward a cavity resonance in the BaTiO₃ crystal.

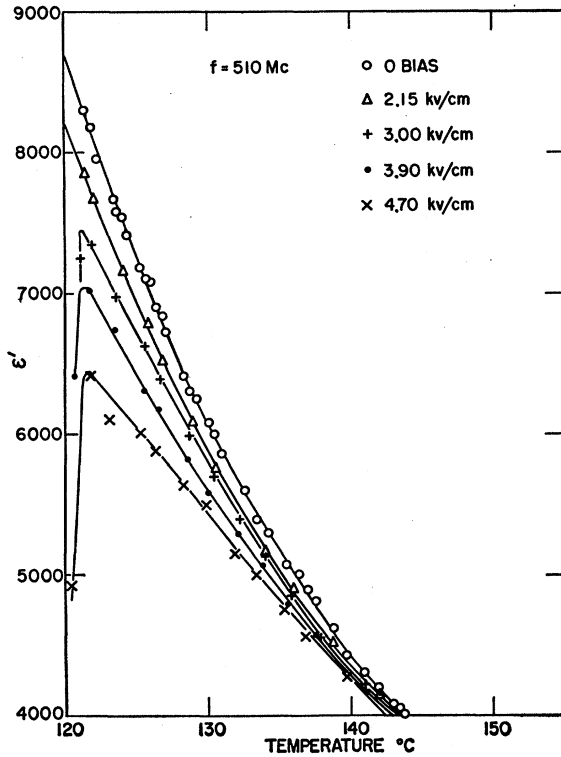


FIG. 10. Relative dielectric constant vs temperature for a number of different biasing voltage.

units near the Curie point, which is indicative of the unclamped condition.

CONCLUSIONS

We have measured the frequency dependence of the complex dielectric constant of BaTiO₃ single crystals with special emphasis on the behavior in the paraelectric region. The measurements at 1 kc/sec are in agreement with previous results. At frequencies above 500 Mc/sec the losses observed are consistent with a series equivalent circuit to represent our electroded BaTiO₃ crystals. In keeping with tradition, it is believed that the origin of this series resistance is at the surfaces. We find in using this model that there is no relaxation of ϵ_0' in the frequency range under study.

The effect of an electric biasing field on the dielectric constant at 500 Mc/sec was also investigated. It is established that the B_F^G coefficient at 500 Mc/sec is positive indicating that the crystal is clamped by the microwave field. The experimental results are in excellent agreement with Devonshires phenomenological equation for BaTiO₃.^{2,4,8}

ACKNOWLEDGMENTS

The authors wish to thank Mr. B. L. Havens for suggesting this research and Professor N. Kroll, Dr. S.

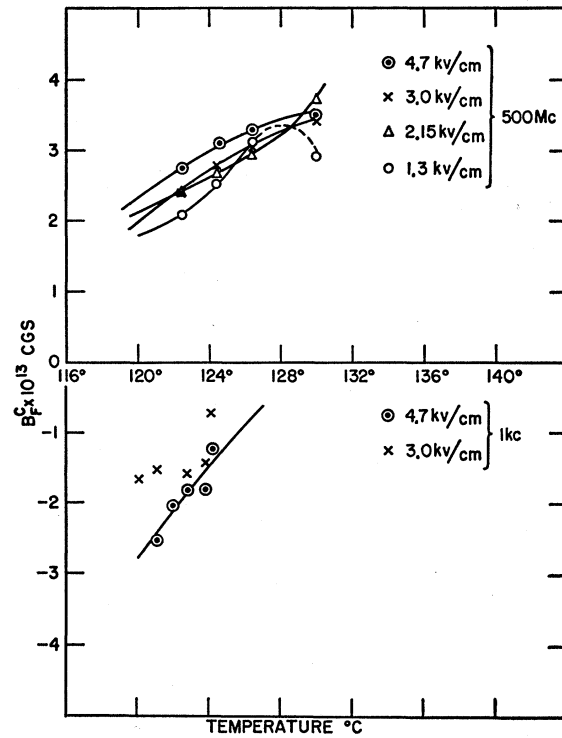


FIG. 11. B_F^G coefficient vs temperature at 1 kc/sec and at 500 Mc/sec.

Triebwasser and M. Drougard for many enlightening discussions. In addition, a conversation with Professor E. T. Jaynes at the beginning of this research about his earlier work on BaTiO₃ was very helpful.

APPENDIX

Derivation of Expression for $\tan\delta$ of Sample

The loss tangent of the sample is defined by the relation

$$\tan\delta_s = (1/Q_s) = (G_s/\omega C_s).$$

Let the Q -meter dial readings be: C_0, Q_0 for Q -meter terminals open; C_1, Q_1 for empty test line connected to terminal; C_2, Q_2 for test line plus sample connected to terminal. It should be noted that since the measuring frequency is held constant:

$$C_1 + C_{\text{line}} = C_0 \quad \text{and} \quad C_2 + C_{\text{line}} + C_s = C_0.$$

Then we have

$$C_s = C_1 - C_2,$$

and

$$Q_2 = [\omega C_0 / (G_0 + G_i + G_s)],$$

so that

$$G_s = (\omega C_0 / Q_2) - (G_0 + G_i) = (\omega C_0 / Q_2) - (\omega C_0 / Q_1),$$

$$\tan\delta_s = [C_0 / (C_1 - C_2)] [(1/Q_2) - (1/Q_1)].$$